



## Molecular sieving carbon catalysts for liquid phase reactions: Study of alkene hydrogenation using platinum embedded nanoporous carbon

Billy Paul M. Holbrook<sup>a</sup>, Ramakrishnan Rajagopalan<sup>b</sup>, Krishna Dronvajjala<sup>c</sup>,  
Yogesh Kumar Choudhary<sup>c</sup>, Henry C. Foley<sup>a,b,c,\*</sup>

<sup>a</sup> Department of Chemistry, University Park, PA 16802, United States

<sup>b</sup> Department of Chemical Engineering, University Park, PA 16802, United States

<sup>c</sup> Materials Research Institute, University Park, PA 16802, United States

### ARTICLE INFO

#### Article history:

Received 27 September 2012

Received in revised form 25 October 2012

Accepted 26 October 2012

Available online 5 November 2012

#### Keywords:

Molecular sieving carbon catalyst

Shape selectivity

Alkene hydrogenation

Transition shape selectivity

Microporous carbon

### ABSTRACT

We present a simple method to synthesize shape selective carbon catalysts for large alkene hydrogenation reactions by tailoring porosity of platinum embedded in polyfurfuryl alcohol derived carbons. A small amount of mesoporosity, in addition to the intrinsic microporous nature of the carbon, shortens the diffusion length for the reactant molecule, enabling these materials to be used for catalysis in the liquid phase. A systematic study of hydrogenation reactions of liquid phase alkenes is reported. The molecular sieving effect of the catalyst was examined by varying molecular length, size, double bond position, stereoregularity and the number of double bonds in the alkenes.

© 2012 Elsevier B.V. All rights reserved.

### 1. Introduction

Shape selective catalysis is used for applications ranging from acid catalyzed hydrocarbon cracking in petroleum manufacture, to the production of monomers such as ethylbenzene, xylene, p-ethyl toluene for polymerization [1]. Currently, zeolites are the only shape selective catalysts to have found wide usage in practice; in addition to their high selectivity for certain reactions, they have adequate to good thermal stability and uniform pore structure. However, there are numerous reactions where the acidic nature of zeolites leads to unfavorable side reactions and deactivation. Thus shape selective catalysis without zeolites is intriguing.

An alternative to shape selective zeolites is molecular sieve carbon (MSC), or nanoporous carbon (NPC) [2–4]. NPC is thermally stable, possesses good mechanical strength and its surface is chemically fungible. In contrast to the inherent surface acidity of zeolites, NPC can be acidic, basic or neutral. That said NPC are complex solids; they are not crystalline, unlike zeolites. In spite of their global disorder, the NPC derived directly from polyfurfuryl alcohol (PFA) has a narrow pore size distribution with an average of about 0.5 nm, much like the ZSM-5 zeolites. Although we lack the kind of ready

and detailed understanding of the origin of their regularly sized pores that we enjoy with zeolites, we are not at a total loss if insight. It is considered most likely that the regular porosity is due to the misalignment of polyaromatic domains in the carbon framework arising from the inclusion of curvature induced by the presence of five and seven membered rings being in close proximity to six membered rings. While this is quite a contrast to the crystalline structure of zeolites their molecular sieving capabilities are similar. Therefore, the NPC materials offer intriguing possibilities for combining catalysis with shape selective effects in the synthesis and production of fine chemicals. It can be imagined that NPC could be found useful and better in such reactions than metals on activated carbon, but only if the metals within them can be made accessible to large molecules for liquid phase reactions and if these metals can be stabilized against sintering.

Catalysis with platinum embedded within nanoporous carbon has been demonstrated in nearly defect-free, platinum-loaded NPC membranes [5–7]. The platinum-containing catalytic membranes displayed significant size selectivity in the hydrogenation of different simple gas phase alkenes. The ratios of the intrinsic rate constants for differently sized light alkenes hydrogenated within these membranes were much more sensitive to the alkene chain length (propylene/isobutylene and 1-butene/isobutylene) than were the same ratios derived for more standard platinum supported on carbon catalysts [7]. Since the analysis of the reaction data had already taken into account the different diffusivities

\* Corresponding author at: Department of Chemical Engineering, University Park, PA 16802, United States. Tel.: +1 814 865 6332; fax: +1 814 865 7846.

E-mail addresses: [hcf2@psu.edu](mailto:hcf2@psu.edu), [hankfoley@enr.psu.edu](mailto:hankfoley@enr.psu.edu) (H.C. Foley).

as a function of size for the alkenes, it was considered likely that the magnitudes of the intrinsic rate constant ratios were a result of the carbon's micropores (average size  $\sim 0.5$  nm) exerting steric effects on the intermediates and possibly even on transition states that led from reactants to products. This hypothesis was bolstered by HRTEM images, which showed that the regular carbon channels extended from the bulk of the carbon matrix to the surface of platinum particles. Hence molecular ingress to and egress from the platinum particles surfaces was only through these carbon channels.

More recently a novel synthetic procedure to embed monodisperse platinum nanoparticles in the matrix of nanoporous carbon was reported [8]. Embedding prevents the particles from sintering even at temperatures as high as  $800^\circ\text{C}$  in flowing hydrogen [8]. Our results show that these catalysts also exhibit shape selectivity effects in the gas phase hydrogenation of light alkenes and that these catalysts were highly active at room temperature. However, given that these reactants were such small molecules, to be of more significant interest in catalytic synthesis of high value fine chemicals, the platinum embedded within NPC catalysts must be active for reactions of larger molecules in the liquid phase. In this paper, we examine the catalytic activities of these platinum embedded within nanoporous carbon catalysts for liquid phase hydrogenation of alkenes to better understand and demonstrate their molecular sieving and how that affects their activity and selectivity.

## 2. Experimental

### 2.1. Materials

Platinum (II) (acetyl acetonate)<sub>2</sub> or Pt(acac), furfuryl alcohol (FA), Triton X-100 and p-toluenesulfonic acid monohydrate (p-TSA) were purchased from Aldrich Co and used without any further purification.

### 2.2. Synthesis of platinum nanoparticles in nanoporous carbon

To 5 mL of furfuryl alcohol was added, a known amount of platinum (II) acetyl acetonate in a 125 mL round bottom flask and the mixture was refluxed for 16 h. This resulted in a black colloidal solution of platinum nanoparticles in furfuryl alcohol. The solution was allowed to cool to room temperature and an additional 5 mL of furfuryl alcohol along with 5 mL of Triton X-100 surfactant, were stirred and placed in an ice bath. Next, 0.4 g of p-TSA was dissolved in 5 mL of Triton X-100 and was added gradually to the colloidal solution using a syringe pump. The polymerization was allowed to continue for 24 h. The resultant viscous solution was poured into a glass vial and maintained at  $40^\circ\text{C}$ ,  $60^\circ\text{C}$  and  $100^\circ\text{C}$  for three consecutive days, respectively. The solidified resin was then pyrolyzed under flowing argon in a quartz tube furnace. The sample was heated to  $200^\circ\text{C}$  over the course of 1 h, maintained at that temperature for 2 h and then was slowly increased to  $800^\circ\text{C}$  at  $2.5^\circ\text{C}/\text{min}$  and thermally "soaked" at  $800^\circ\text{C}$  for 8 h. The exact amount of platinum embedded into the carbon was calculated using the final weight of the carbon and initial weight of platinum (II) acetylacetonate. The catalyst was crushed and sieved to particles ranging in size from 90 to  $180\ \mu\text{m}$ . Pretreatment of the catalyst was done in a quartz tubular flow reactor by heating to  $800^\circ\text{C}$  under UHP argon. At  $800^\circ\text{C}$ , a mixture of UHP argon and hydrogen (70:30) was introduced into the reactor and the catalyst was reduced under these conditions for 3 h. The catalyst was then slowly brought down to room temperature under flowing argon atmosphere. This catalyst will be referred as Pt-PFA-TX in the manuscript.

Platinum embedded nanoporous carbon catalysts were prepared using tetrahydrofuran (THF) as diluent instead of Triton X-100. We used a procedure nearly identical to that described above to make these catalysts. This catalyst was labeled as Pt-PFA-THF. In addition to the synthesized catalysts, a standard 10 wt.% platinum catalyst dispersed on the surface of carbon black was purchased from Alfa Aesar Co. and used as a control for the hydrogenation reactions.

### 2.3. Transmission electron microscopy (TEM)

The images of platinum embedded nanoporous carbon were examined using an Hitachi HF2000 high resolution transmission electron microscopy. In addition to the high-resolution images, the size of the platinum nanoparticles was calculated using images taken by HD2000 scanning transmission electron microscopy.

### 2.4. Scanning electron microscopy

Surface topography of the samples was studied using ultra high resolution low KV Hitachi S-5200 microscope. The morphologies of the samples were studied and the dispersion of platinum was confirmed by taking the back-scattered images of the samples.

### 2.5. Pore size distribution

The total pore volume and the average pore size were calculated from methyl chloride adsorption isotherms using the Horvath–Kawazoe slit shape pore model [9]. Before the methyl chloride adsorption, the catalyst was heated to  $350^\circ\text{C}$  and held there for 4 h under vacuum. The catalyst was then allowed to cool to room temperature and then the adsorption isotherm was measured based on gravimetric uptake of methyl chloride at different pressures. Typically, the uptake equilibration time was between 2 and 3 h at each pressure. The adsorption isotherm was measured at 273 K, 295 and 304 K for the pressure range of 5–700 Torr.

### 2.6. Hydrogen chemisorption

0.3 g of the catalyst was loaded into a Micromeritics Autochem II chemisorption unit. The catalyst was pretreated at  $400^\circ\text{C}$  under a helium atmosphere. This was followed by reduction under 1 atm of hydrogen at  $400^\circ\text{C}$  for 1 h. The sample was then cooled to  $350^\circ\text{C}$  and the cell was evacuated for half hour. The pretreated sample was brought to room temperature and the chemisorption was carried out. The volume of the sample cell was calibrated using helium gas.

### 2.7. Study of liquid phase olefin hydrogenation

0.5 g of catalyst were reduced under flowing UHP hydrogen at  $130^\circ\text{C}$  in a low-pressure stirred reactor (PARR 5100) for 1 h. The reactor was pressurized to 3 bar with UHP hydrogen and allowed to cool to room temperature overnight. After depressurizing the reactor, a 50 mL reactant mixture containing 40 mL of undecane (solvent) and 10 mL of the reactant was added. The vessel was then pressurized to 4 bars with hydrogen and the temperature was maintained at  $30^\circ\text{C}$ . The products were analyzed using GowMac 600 series GC using a flame ionization detector and xTi-5 column from Restek.

Care was taken to ensure that the reaction was not externally mass transfer controlled by making sure that the rate of mixing, modified by changing the speed of rotation of the impeller did not have any impact on the observed reaction rate. Turnover frequency number was reported for each reaction as the ratio of

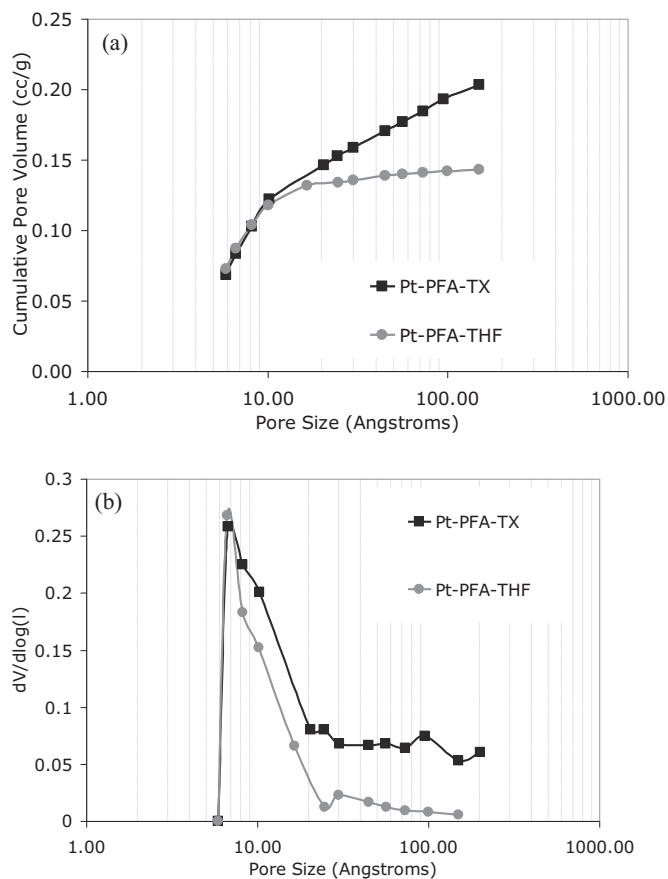


**Fig. 1.** (a) Cumulative pore volume of 12 wt.% Pt-PFA-TX and 12 wt.% Pt-PFA-THF and (b) pore size distribution of 12 wt.% Pt-PFA-TX and Pt-PFA-THF as measured using methyl chloride adsorption tests.

**Table 1**

Mesopore and micropore size distribution of the synthesized platinum embedded catalyst as measured using methyl chloride adsorption tests.

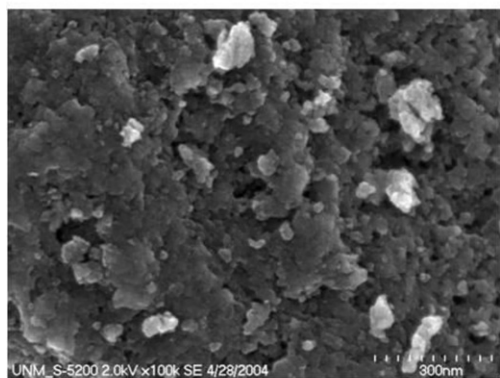
Catalyst	$V_{\text{micro}}$ (cc/g)	$V_{\text{meso}}$ (cc/g)	$V_{\text{Total}}$ (cc/g)
12 wt.% Pt-PFA-THF	0.18	0.06	0.24
12 wt.% Pt-PFA-TX	0.15	0.01	0.16
Control	0.33	0.19	0.52

observed reaction rate to the number of active sites measured using chemisorption.

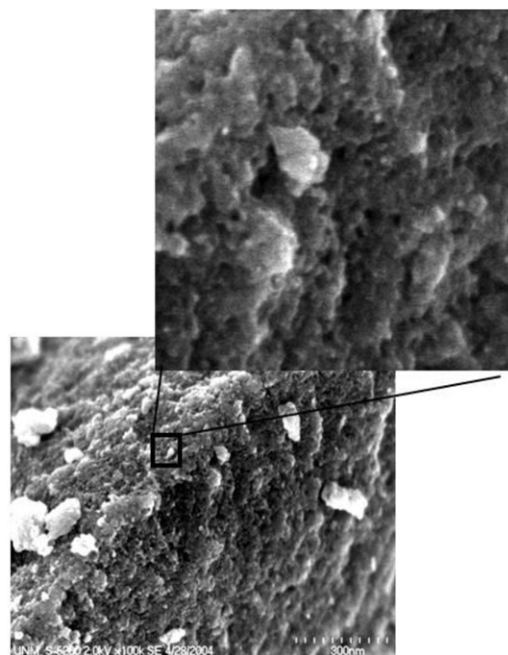
### 3. Results

#### 3.1. Synthesis and characterization of platinum embedded nanoporous carbon catalysts

In our previous investigation, we reported the synthesis of well-dispersed platinum nanoparticles sequestered within a matrix of nanoporous carbon [1]. During the synthesis of the catalyst, we added Triton X-100 as a surfactant to disperse the nanoparticles. However, when a large volume of Triton X-100 (1:1 by volume with furfuryl alcohol) was added, it also began to act as a pore former. Table 1 shows the cumulative micro- and mesopore volume of 12 wt.% platinum embedded carbon made by the pyrolysis of platinum nanoparticles/polyfurfuryl alcohol composites that were synthesized using THF and Triton X-100 as diluent, respectively. The porosity of the Pt-PFA-THF catalyst was predominantly microporous ( $\sim 0.15$  cc/g) with pore sizes less than 2 nm as shown in Fig. 1. By contrast, Pt-PFA-TX had both the micropore (<2 nm) and mesopores (2–50 nm). The micropore volume of Pt-PFA-TX was similar ( $\sim 0.18$  cc/g) while the mesopore volume was almost six times more than the Pt-PFA-THF catalyst ( $\sim 0.06$  cc/g). Commercial 10 wt.% platinum impregnated catalyst had significant amount of micropore and mesopore volume.



(a)



(b)

**Fig. 2.** Low kV high resolution scanning electron micrograph of (a) nanoporous carbon derived from polyfurfuryl alcohol and (b) 12 wt.% Pt-PFA-TX.

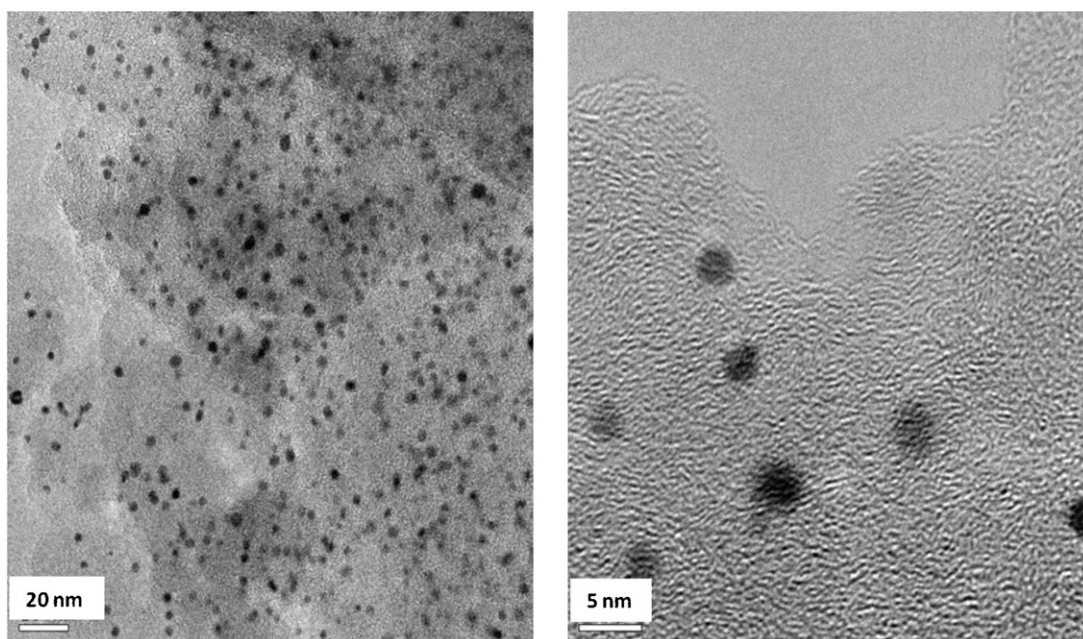


**Fig. 3.** (a) HRTEM image of 12 wt.% Pt-PFA-TX and (b) an enlarged image of platinum nanoparticles submerged in the nanoporous carbon matrix.

The surface topography of platinum embedded carbon was examined using a low KV high resolution SEM. Nanoporous carbon made with polyfurfuryl alcohol had relatively smooth morphology as shown in Fig. 2. In contrast, the Pt-PFA-TX had a porous texture. The presence of 10 nm pores was evident in the 12 wt.% Pt-PFA-TX.

Transmission electron microscopy and XRD studies showed that the platinum nanoparticles were well dispersed in all samples and that the average particle size was about 3–4 nm as shown in Fig. 3.

### 3.2. Hydrogen chemisorption

Table 2 summarizes the results of hydrogen uptake as calculated from the data obtained from the hydrogen chemisorption experiments. The results show that the apparent number of available active sites for chemisorption is low. The amount of hydrogen uptake did increase with increase in platinum loading, but the apparent dispersion of catalytic active sites was invariant with loading and was nominally about 4%. The dispersion of platinum loaded on carbon black (control) was about 13.6%.

### 3.3. Catalytic activity of platinum embedded carbon

In order to probe the reactant size selectivity for the alkenes, the hydrogenation reactions were done under similar conditions. The catalysts showed excellent size selectivity and the reactivity decreased with increase in the size of the reactant molecules (1-hexene < 1-octene < 1-nonene < 1-decene) as shown in Fig. 4. Hydrogenations of 1-hexene, 2-hexene and 3-hexene showed that the activity of reactant was highly dependent on the position of the double bond. When the double bond was moved toward the inner

**Table 2**  
Hydrogen chemisorption results of platinum embedded nanoporous carbon catalysts.

Catalyst	H <sub>2</sub> uptake (μmol/g)	Dispersion
4 wt.% Pt-PFA-TX	4.19	4
6 wt.% Pt-PFA-TX	6.65	4
12 wt.% Pt-PFA-TX	11.10	4
20 wt.% Pt-PFA-TX	12.93	3
Control	35	13.6

most position along the alkyl chain, the reactivity decreased. The order of reactivity was as follows: 1-hexene > 2-hexene > 3-hexene (Fig. 5).

We probed the effect of steric hindrance on the double bond of the olefins by performing hydrogenation reactions of 1-hexene, 2-methyl-1-pentene, 3-methyl-1-pentene and 4-methyl-1-pentene using both control and our catalyst as shown in Fig. 6. In the case of commercial catalyst (control), all the reactants, 2-methyl-1-pentene, 3-methyl-1-pentene and 4-methyl-1-pentene, hydrogenated completely within 60 min. The reactivity for all the reactants was very similar, regardless of the placement of the alkyl groups. However, the reactivity of the alkenes with the embedded catalysts was significantly affected by the proximity of the methyl groups to the unsaturated double bond. Here 2-methyl-1-pentene was far less reactive than 3-methyl-1-pentene, 4-methyl-1-pentene and 1-hexene, demonstrating the severe steric hindrance effect. Furthermore, 3-methyl-1-pentene had a higher reactivity than 4-methyl-1-pentene. A significant

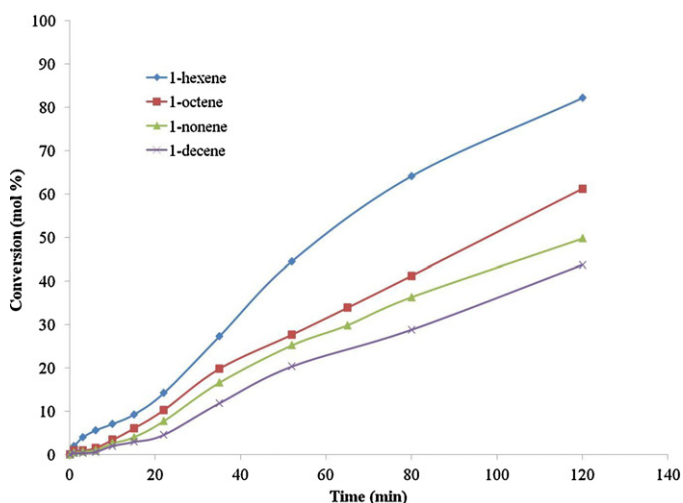


**Fig. 4.** Study of hydrogenation reactions using 12 wt.% Pt-PFA-TX catalyst as a function of length of the reacting olefins.

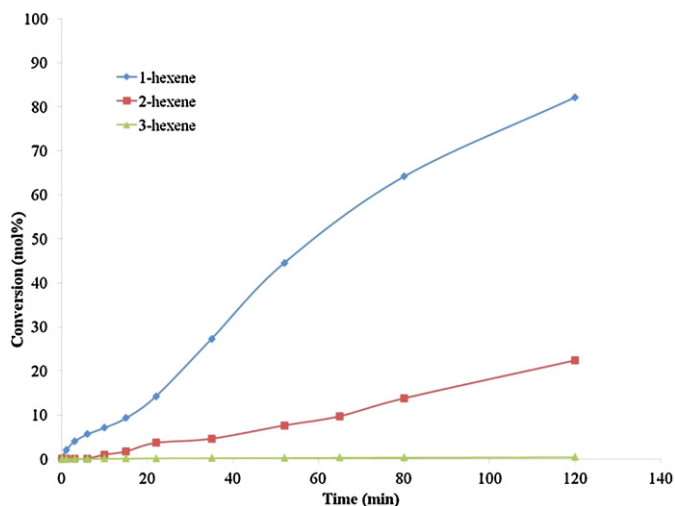


**Fig. 5.** Study of hydrogenation reactions as a function of position of double bond in the reacting olefins using 12 wt.% Pt-PFA-TX.

effect of stereoregularity on the extent of hydrogenation of the reactant molecules was also observed for trans-2-hexene and cis-2-hexene. A comparison of their reactivities showed that the cis-2-hexene was far less reactive than the trans-2-hexene (Fig. 7).

Hydrogenation of a diene molecule such as 1,5-hexadiene using 12 wt.% Pt-PFA-TX was compared with a control catalyst (Fig. 8). Both the catalysts showed two main products namely 1-hexene (intermediate product) and n-hexane. As expected, the reactivity of the control catalyst was greater than the embedded platinum catalyst. The reaction went to 100% conversion within 1 h of reaction time over the control catalyst whereas over Pt-PFA-TX, it took almost 48 h to undergo complete conversion. Although the reaction was fast over the control catalyst, the selectivity of 1-hexene/n-hexane was always less than unity, even at low conversions and was 0.01 at 95% conversion. However, due to the shape selective nature of Pt-PFA-TX, we saw that the selectivity of 1-hexene/n-hexane was greater than unity up to 40% conversion and fell to 0.3 at 95% conversion (Fig. 9).

Table 3 summarizes the performance of the catalyst for various alkene hydrogenation reactions.

#### 4. Discussion

Our objective in this investigation was to examine whether or not we could extend the development of shape selective carbon catalysts previously reported, to liquid phase reactions [8]. We began

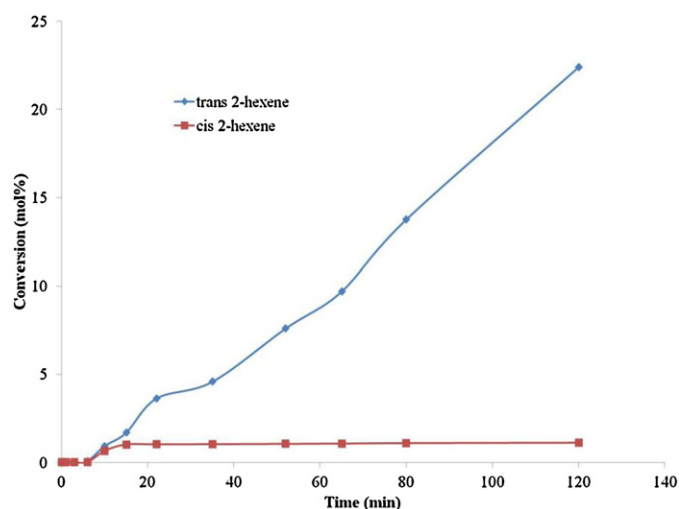


**Fig. 7.** Study of hydrogenation reactions using 12 wt.% Pt-PFA-TX as a function of stereoregularity.

**Table 3**

Catalytic turnover frequencies for hydrogenation reactions of different alkenes over the platinum embedded nanoporous carbon catalysts (Pt-PFA-TX).

Type of olefin	12 wt.% Pt-PFA-TX TOF ( $s^{-1}$ )	10 wt.% Pt control TOF ( $s^{-1}$ )
1-Hexene	0.75	0.32
Trans-2-hexene	0.20	0.32
Trans-3-hexene	0.004	0.32
Trans 4-methyl-1-pentene	0.076	0.32
Trans 3-methyl-1-pentene	0.53	0.32
Trans 2-methyl 1-pentene	0.43	0.32
1-Octene	0.44	–
1-Nonene	0.32	–
1-Decene	0.29	–

our studies by looking at the pore size distribution of the catalysts. In order to facilitate transport of liquid reactants and products, it is required to create mesoporosity in addition to the inherent nanoporous nature of polyfurfuryl alcohol derived carbon.

Previously, the evolution of porosity in polyfurfuryl alcohol was reported [10]. It was shown that most of the gaseous by-products were released between 300 °C and 500 °C. Porosity in these materials formed as soon as the decomposition of the polymer began. However, when pyrolysis was done at temperatures greater than 500 °C, the mesoporosity so formed collapsed due to the annealing of the aromatic domains, leaving behind a nanoporous carbon.

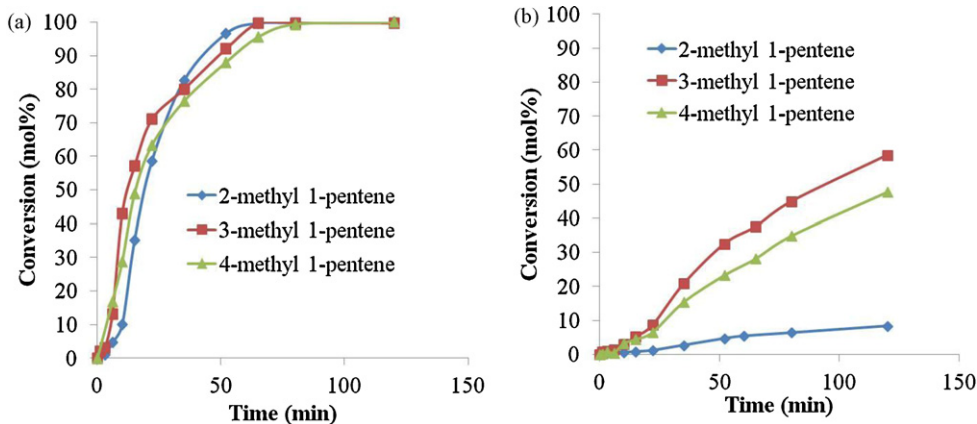


**Fig. 6.** Study of hydrogenation reactions using (a) control and (b) 12 wt.% Pt-PFA-TX as a function of proximity of methyl groups to the double bond in the reacting olefins.

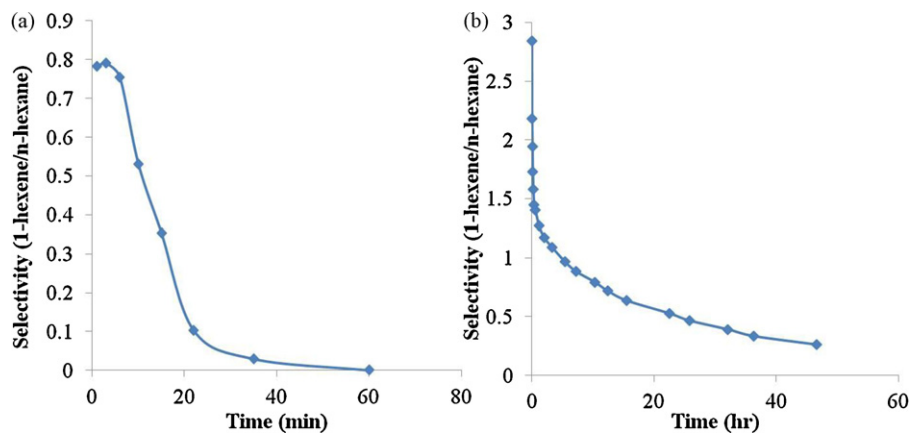


Fig. 8. Study of hydrogenation reaction of 1,5-hexadiene using (a) control and (b) 12 wt.% Pt-PFA-TX.

It was concluded that this behavior could be changed if a pore-forming molecule was added to the mixture as an additive during the pyrolysis. This objective was easily accomplished by using the surfactant molecule, Triton X-100, during the synthesis of the platinum embedded in polyfurfuryl alcohol. The presence of Triton X-100 during pyrolysis created mesoporosity in the carbon that was retained even after annealing at 800 °C for 8 h. This mesoporosity reduced resistance offered by the native PFA-derived carbon to the transport of the reactant molecules, while preserving the shape selective nature of the catalyst due to the presence of nanopores in the immediate vicinity of the highly reactive platinum nanoparticles. As reported previously, we saw that the catalysts prepared using this method had very high resistance to sintering [8].

Hydrogen chemisorption experiments showed very little hydrogen uptake. The apparent dispersion of catalytic sites on the basis of hydrogen chemisorption was about 4% and was invariant with loading. The maximum theoretical dispersion for a 3–4 nm particle, if it were supported on the surface of an activated carbon and if it were completely accessible to hydrogen would be about 28%. The deviation between expected and measured is a factor of seven. All the platinum particles are completely embedded within the nanoporous carbon; however, hydrogen can access only those platinum particles that are accessible in the porous sections of the carbon. Therefore we cannot measure the dispersion accurately by hydrogen chemisorption because many of the platinum particles are inaccessible to hydrogen. However, despite being inaccessible, we include their mass in the calculation of the measured dispersion

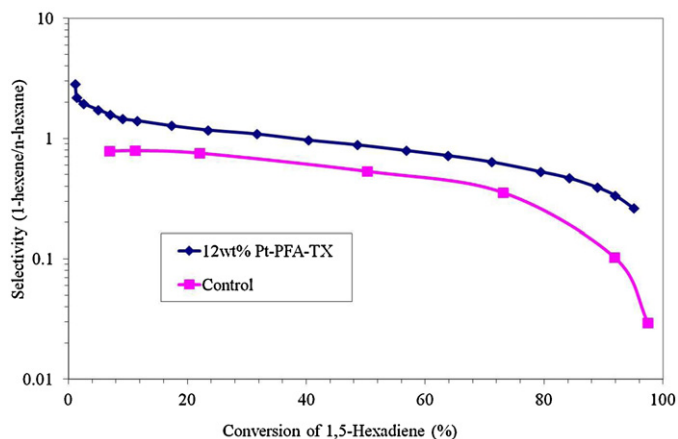


Fig. 9. Selectivity of 1-hexene/n-hexane formed during hydrogenation of 1,5-hexadiene using (a) 12 wt.% Pt-PFA-TX and (b) control.

of 4% and this drops that value of the dispersion by a factor of seven or more below expectation.

We can get at this in another way to confirm the explanation by considering the actual porosity of the NPC. The available micropore volume in these materials is about 0.15–0.18 cm<sup>3</sup> g<sup>-1</sup> and the total pore volume for Pt-PFA-THF and Pt-PFA-TX was about 0.16 cm<sup>3</sup> g<sup>-1</sup> and 0.24 cm<sup>3</sup> g<sup>-1</sup>, respectively. The accessible porosity calculated based on the fraction of void volume to the total volume occupied by the catalyst amounts to 25% and 33%, respectively. As the platinum is evenly dispersed within the carbon, almost 75% of the platinum is in the non-porous regions of the carbon and is rendered inaccessible. Thus given that the maximum theoretical dispersion for 3–4 nm platinum particles should have been about 25%, if one third to one fourth of the platinum is accessible, then the apparent dispersion due to this effect could be no better than 6.25–8.25%. Moreover, it has also been shown that the platinum surface can be contaminated by carbon and can result in lower dispersion [11–13]. We measured dispersion of 4%. This result is in good agreement with the expected value when we factor in the actual porosity of the NPC and carbon contamination on the surface. It is interesting to note that the turnover frequencies for these catalysts (see Table 3) are quite high.

The next objective was to clearly demonstrate the molecular sieving nature of the platinum embedded in carbon catalyst by doing liquid phase hydrogenation reactions. The reactions were varied on the basis of molecular size and shape, on the position of double bond, on stereoregularity and number of double bonds in the reactant molecule. There have been extensive investigations using single crystal studies on platinum aimed at elucidating the actual mechanism of hydrogenation of alkenes [14–17]. It has been shown that alkenes may be adsorbed either by forming a strong  $\sigma$ -bond or a weak  $\pi$ -bond with the single crystal surface of platinum. Spectroscopic studies showed that the  $\sigma$ -bonded alkenes do not participate in the hydrogenation and it is believed that the weakly  $\pi$ -bonded alkenes on the Pt (1 1 1) crystal are the ones that undergo hydrogenation. If in fact the  $\pi$ -bond formation is critical, then the reactant molecule should sit parallel to the platinum surface. This results in an interesting conformational problem in these embedded platinum catalysts as the pores of the carbon are on average only 0.5 nm and these surround the catalyst particles and extend to their surfaces. Our hydrogenation results confirm this effect.

In the hydrogenation of alkenes that have kinetic diameters ranging from 0.5 nm (n-hexene) to 0.8 nm (n-octene), the reactivity decreased with the increase in the chain length of the reacting alkene. We also explored the effect of more subtle variations such as the presence of steric hindrance due to

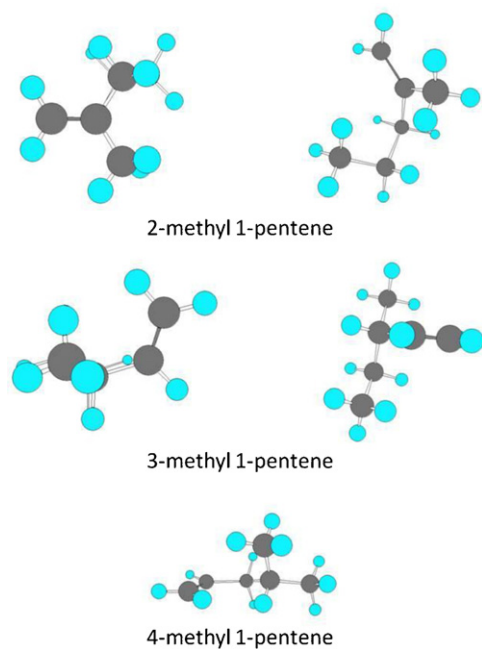


**Fig. 10.** Structural models of (a) 2-methyl-1-pentene, (b) 3-methyl-1-pentene and (c) 4-methyl-1-pentene.

methyl groups near the double bond of the alkenes. We compared our catalyst with a standard catalyst that supports platinum on the surface of carbon. The reactivities of 2-methyl-1-pentene, 3-methyl-1-pentene and 4-methyl-1-pentene were very similar over the control catalyst. However, comparison of these hydrogenation reactions on the embedded platinum catalyst showed that reactivity of 1-hexene > 3-methyl-1-pentene > 4-methyl-1-pentene > 2-methyl-1-pentene. The transport limitation due to the presence of molecular sieving in addition to the conformational restraint on the alkenes, gives rise to differences in the reactivity for hydrogenation of the alkenes as shown in Fig. 10. In the case of 1-hexene, three hydrogens and alkyl groups surround the double bond. This facilitates the double bond making it to the surface as the alkyl groups move either up or, out, away from the surface. By contrast 2-methyl-1-pentene has a methyl and propyl group totally out of plane with the double bond making it more difficult for the double bond to align parallel to the catalyst surface. For 3-methyl-1-pentene and 4-methyl-1-pentene, although the branched methyl group is closer to the double bond, in 3-methyl-1-pentene versus 4-methyl-1-pentene, the double bond reacts faster. Considering structures, the double bond in 3-methyl-1-pentene is out of plane with respect to all other carbon atoms allowing the double bond to come into close proximity with the platinum particle surface as compared to the double bond in the 4-methyl-1-pentene.

We also looked at the effect of stereoregularity by comparing trans-2-hexene and cis-2-hexene. For trans-2-hexene, there is less resistance as the molecule moves through the pores of the carbon to the catalytic site. By comparison cis-2-hexene has a less streamlined structure that increases resistance to transport through the porous carbon as shown in Fig. 11.

The effect of having multiple double bonds in the molecule was probed using 1,5-hexadiene. Once again we compared the performance of the embedded catalysts with the control catalyst in which platinum is dispersed on the carbon surface. For both catalysts, the same two products, 1-hexene and 1-hexane were observed. The transport resistance in the embedded platinum catalyst was evidenced by its slower rate of hydrogenation when compared to the control. But, it was also interesting to note that the

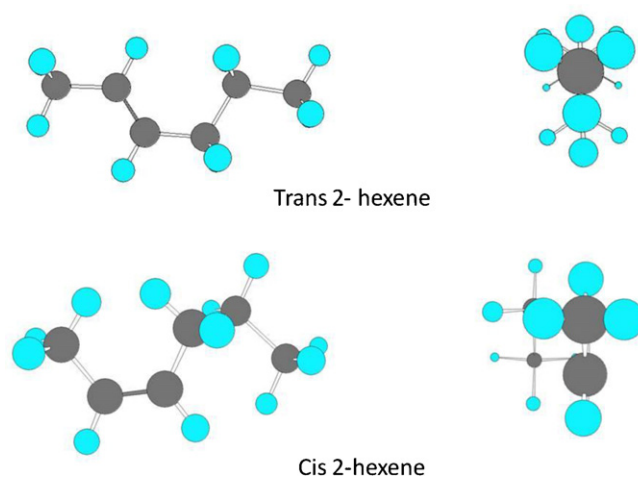


**Fig. 11.** Structural models of (a) trans-2-hexene and (b) cis-2-hexene.

selectivities of 1-hexene/1-hexane were different for the two catalysts. In the case of the standard catalyst, the selectivity of 1-hexene/hexane was less than one even at very low conversions (<10%), while for the embedded platinum catalyst this ratio was greater than one for conversions as high as 40% conversion. This may be evidence of a transition state shape selective effect. Furthermore, at very high conversions, we see that the selectivity ratio drops precipitously for standard catalyst (0.01), while it remains at about 0.3 even at 95% conversion with the embedded catalyst.

## 5. Conclusions

In this investigation, we show that molecular sieving carbon catalysts can be synthesized for liquid phase hydrogenation reactions by pyrolyzing platinum nanoparticles in PFA resulting in platinum embedded in PFA-carbon nanocomposites. The porosity of the carbon can be improved significantly by using a mesopore former such as Triton X-100 during the synthesis of the polymer precursor and during its subsequent pyrolysis. Steric and conformational restriction effects on size and shape selectivity of the catalysts were demonstrated using several different liquid phase alkene hydrogenation reactions. Based on these findings molecular sieving carbon catalysts can be developed further for reactions that are important to the biological, pharmaceutical and fine chemical industries.

## Acknowledgments

We would like to acknowledge Dr. Larry Allard at Oakridge National Laboratory for assisting us with HRTEM images. We would also like to thank Prof. Abhaya Datye, University of New Mexico for helping us characterize the catalysts using low KV high resolution Scanning Electron Microscopy.

## References

- [1] S.M. Csicsery, *Pure Appl. Chem.* 58 (1986) 841.
- [2] J.L. Schmitt, P.L. Walker Jr., *Carbon* 9 (1971) 791.
- [3] J.L. Schmitt, P.L. Walker Jr., *Carbon* 10 (1972) 87.
- [4] D.L. Trimm, B.J. Copper, *J. Catal.* 31 (1973) 287.
- [5] D.S. Lafyatis, R.K. Mariwala, E.E. Lowenthal, H.C. Foley, in: M.L. Occelli, H. Robson (Eds.), *Design and Synthesis of Carbon Molecular Sieves for Separation and Catalysis*, Van Nostrand Reinhold, New York, 1992, pp. 318–332.
- [6] K. Miura, J. Hayashi, T. Kawaguchi, K. Hashimoto, *Carbon* 31 (1993) 667.
- [7] M.S. Strano, H.C. Foley, *AIChE J.* 47 (2001) 66.

- [8] R. Rajagopalan, A. Ponnaiyan, P.J. Mankidy, A.W. Brooks, B. Yi, H.C. Foley, *Chem. Commun.* 21 (2004) 2498.
- [9] R.K. Mariwala, H.C. Foley, *Ind. Eng. Chem. Res.* 33 (1994) 2314.
- [10] C.L. Burket, R. Rajagopalan, A.P. Marencic, K. Dronavajjala, H.C. Foley, *Carbon* 44 (2006) 2957.
- [11] N. Krishnankutty, M.A. Vannice, *J. Catal.* 155 (1995) 312.
- [12] N. Krishnankutty, M.A. Vannice, *J. Catal.* 155 (1995) 327.
- [13] H. Chen, H. Yang, Y. Briker, C. Fairbridge, O. Omotoso, L. Ding, Y. Zheng, Z. Ring, *Catal. Today* 125 (2007) 256.
- [14] P.S. Cremer, X. Su, Y.R. Shen, G.A. Somarjai, *J. Am. Chem. Soc.* 118 (1996) 2942.
- [15] A.L. Marsh, G.A. Somarjai, *Top. Catal.* 34 (2005) 121.
- [16] D. Chrysostomou, C. French, F. Zaera, *Catal. Lett.* 69 (2000) 117.
- [17] I. Lee, F. Zaera, *J. Phys. Chem. B* 109 (2005) 2745.